ELSEVIER

Fuel 79 (2000) 1725–1742

FUEL

www.elsevier.com/locate/fuel

Black Sea sapropels: relationship to kerogens and fossil fuel precursors

S.D. Brown[a], G. Chiavari[b], V. Ediger[c], D. Fabbri[d], A.F. Gaines[a,*], G. Galletti[b], A.I. Karayigit[e], G.D. Love[a], C.E. Snape[a,1], O. Sirkecioglu[a], S. Toprak[f]

[a]*University of Strathclyde, Department of Pure and Applied Chemistry, Thomas Graham Building, 295 Cathedral Street, Glasgow G1 1XL, Scotland, UK*
[b]*Dipartimento di Chimica "G.Ciamician", Universita di Bologna, via G. Selmi 2, I-40126 Bologna, Italy*
[c]*Institute of Marine Sciences, Middle East Technical University, PO Box 28, Erdemli 33731, Icel, Turkey*
[d]*Dipartimento di Chimica e Labortario di Chimica Ambientale, Universita di Bologna, via Marconi 2, I-48100 Ravenna, Italy*
[e]*Hacettepe University, Department of Geological Engineering, Beytepe, Ankara, Turkey*
[f]*Directorate of Mineral Research and Exploration (MTA), Ankara, Turkey*

Received 10 March 1999; received in revised form 20 January 2000; accepted 27 January 2000

Abstract

The organic structures in sapropels sampled from two cores obtained at known locations beneath the southern Black Sea have been characterised. Fluorescence petrography shows the sapropels to occur as layers of impure alginite, ~50 μm thick, within Unit 2 of the sediments. Solid state ^{13}C NMR indicates the bulk chemical structures to be very similar to those in an immature Type 1 kerogen (lamosite) oil shale with an aromaticity of ~0.2. Consistent with the immaturity of the sapropels, which are between 3000 and 7000 years old, temperature programmed reduction showed aliphatic and aromatic sulphides to be the major organic sulphur forms. Alkanes formed from phytoplankton lipids, alkyl benzenes, alkyl naphthalenes and some phenols dominated the mix of volatile compounds identified by pyrolysis-gas chromatography/mass spectrometry. About half of the sapropels remained as an involatile, tarry residue after pyrolysis. The structure of the sapropels is consistent with their formation resulting from marine phytoplankton with only small terrigeneous inputs. Future catagenesis may be expected to decarboxylate the lipids, increase the aromaticity and to dry and compress the muds to form a source rock.

Keywords: Sapropels; Kerogen; Black Sea; Alginite; Marinite; Petrography

1. Introduction

About one hundred years ago the term sapropel—and such derivatives as sapropelith—was used to refer to oil shales and Boghead or algal coals containing significant remains of algae or plankton usually deposited in stagnant water [1]. The term connoted an association with oil-forming geochemicals. 'Sapropel' continues to be used to describe certain coals, peats, oil shales and marine sediments though the current definition of the term appears to vary with its context (Refs. [2–6] provide recent examples involving coal, peat, and marine and lacustrine sediments). Thus, the 'sapropels' found in sediments below the Mediterranean and Black seas are traditionally defined merely as black muds, more than 1 cm thick, being part of a pelagic sediment sequence and containing more than 2% of organic carbon [7]. It is the aim of these studies to clarify this definition by determining the composition of the organic material in these sediments so as to relate them both to their deposition and to kerogens or oil precursors. Here the structures of sapropels found in two gravity cores from the southern Black Sea are discussed.

The organic muds (sapropels) comprising those sediments below the Black Sea which became termed 'Unit 2' [8], have been observed to consist of annual layers of fine heterogeneous sapropel–varve couples containing partially fossilised material (e.g. Ref. [9]). Soluble material has been studied by gas chromatography/mass spectrometry [10–13], but in fact, very little material is soluble; Black Sea sapropels are largely kerogen. Infra red spectra [14] showed the sapropels to be predominantly aliphatic and this has been confirmed by pyrolysis-gas chromatography/mass spectrometry (Py.-g.c./m.s.) [15,16], which demonstrated the importance of alkanes and alkenes in the products.

After describing the environment and deposition of the sapropels in the Black Sea, the first petrographic description

* Corresponding author. Tel.: + 44-0141-548-2282; fax: + 44-0141-548-4822.

[1] Present address: School of Chemical, Mining and Environmental Engineering, University of Nottingham, University Park, Nottingham NG7 2RD, UK.

0016-2361/00/$ - see front matter
PII: S0016-2361(00)00031-4

is presented of Black Sea sapropels in which their fluorescence is emphasised. Having thus defined the sapropels and shown them to be impure, relatively unstructured alginites, elemental analyses are provided and the bulk structural characteristics of the kerogen are described as disclosed by ^{13}C nuclear magnetic resonance (NMR) spectrometry, the high pressure temperature programmed reduction (t.p.r) of organic sulphur forms and Py.-g.c./m.s. (including pyrolysis in the presence of tetramethyl ammonium hydroxide). The ^{13}C NMR spectra have provided the average structure of the alginite (marinite) sheets. Py.-g.c./m.s. has elucidated the various classes of compound now present in the alginite and permits a comparison of the structure of alginite with the structures of other liptinite macerals. T.p.r. provides the speciation of those organic sulphur forms in the alginite which can be significant in regulating the formation of crude oil.

Since sapropels have frequently been associated with the generation of crude oil, the results of the investigation of Black Sea sapropels have been compared with the results of similar measurements performed on a lacustrine, Type 1 kerogen oil shale (Goynuk, Oligocene) formed on the edge of the Anatolian plateau—whose geology and chemistry have been well-characterised [17]. This confirms the sapropel kerogen as being the precursor of a source rock.

2. The study area: sapropels in the Black Sea environment

Fig. 1 describes the gravity cores and shows the depths from which the sapropel samples were obtained. Fig. 2, a map of the Black Sea, shows the locations of the cores. Conventionally, visual inspection of the Holocene sediments in cores from beneath the Black Sea divides them into Units 3, 2 and 1, there being a Transition Layer between Units 2 and 1. The organic component of the deepest of the sediments, Unit 3, indicates that during the deposition of these sediments the Black Sea was essentially an oxic and presumably rather shallow, fresh-water lake (Ref. [18] and references therein). At a ^{14}C date of 7700–7000 B.P., the thawing of the prevailing climatic glacial led to a rather sudden advent of Mediterranean water through the Bosphorus. In accord with these observations [18] this caused the abrupt termination of Unit 3 and the initiation of Unit 2 composed of an apparently annual deposition of what are now sapropel–varve couples interspersed with turbidite layers. The annual depositions are contiguous throughout Unit 2 so that the sapropel is several centimetres thick (Fig. 1). It is not clear how well the initial inflow of Mediterranean waters mixed with the fresh water or when the Mediterranean waters commenced to form a layer of denser bottom water. Previous authors have suggested the deposition of Unit 2 to have been predominantly marine [12], though terrigeneous material may have been introduced by rivers or have been provided by the living vegetation covered by brackish water as the Mediterranean intruded. The Mediterranean has usually been infertile and a major role of the rivers that continued to enter the Black Sea must have been to transport inorganic nutrient to nourish annual phytoplankton growth. Then, as now, the river basin would have been larger than the Black Sea itself and the thawing of the glacial probably increased the flow of river water and thus the flux of nutrients [19] into the sea. The growth of phytoplankton this occasioned caused large-scale eutrophication in which the decay of organic matter produced anoxia in the bottom waters. The development of

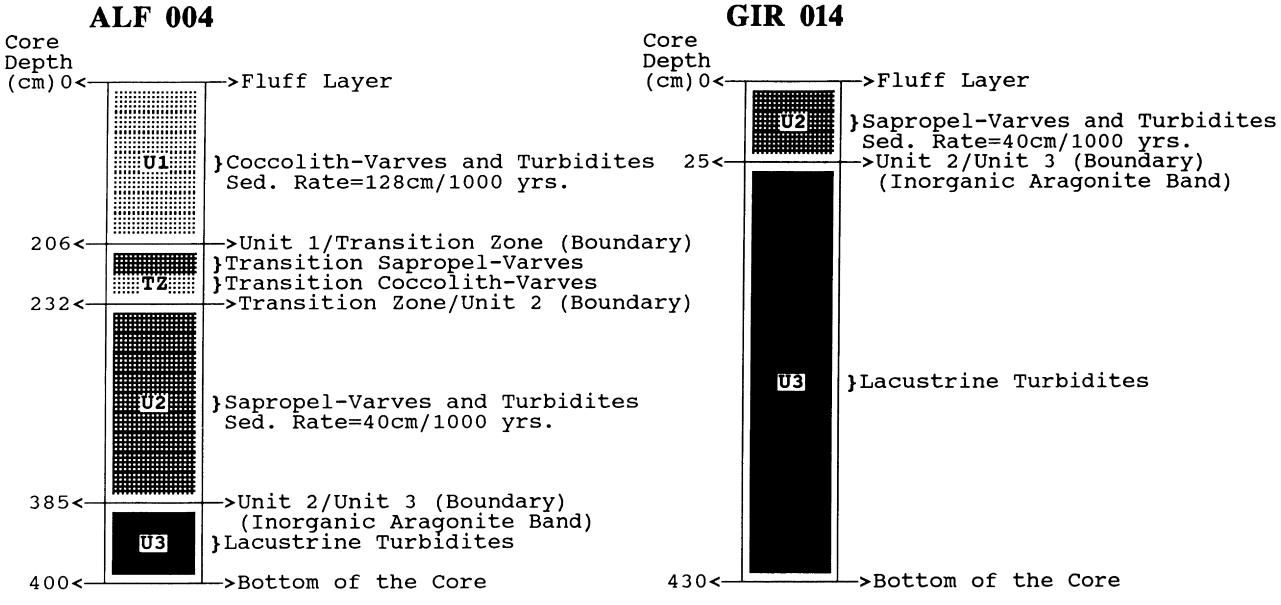

Fig. 1. Description of cores ALF-004 and GIR-014.

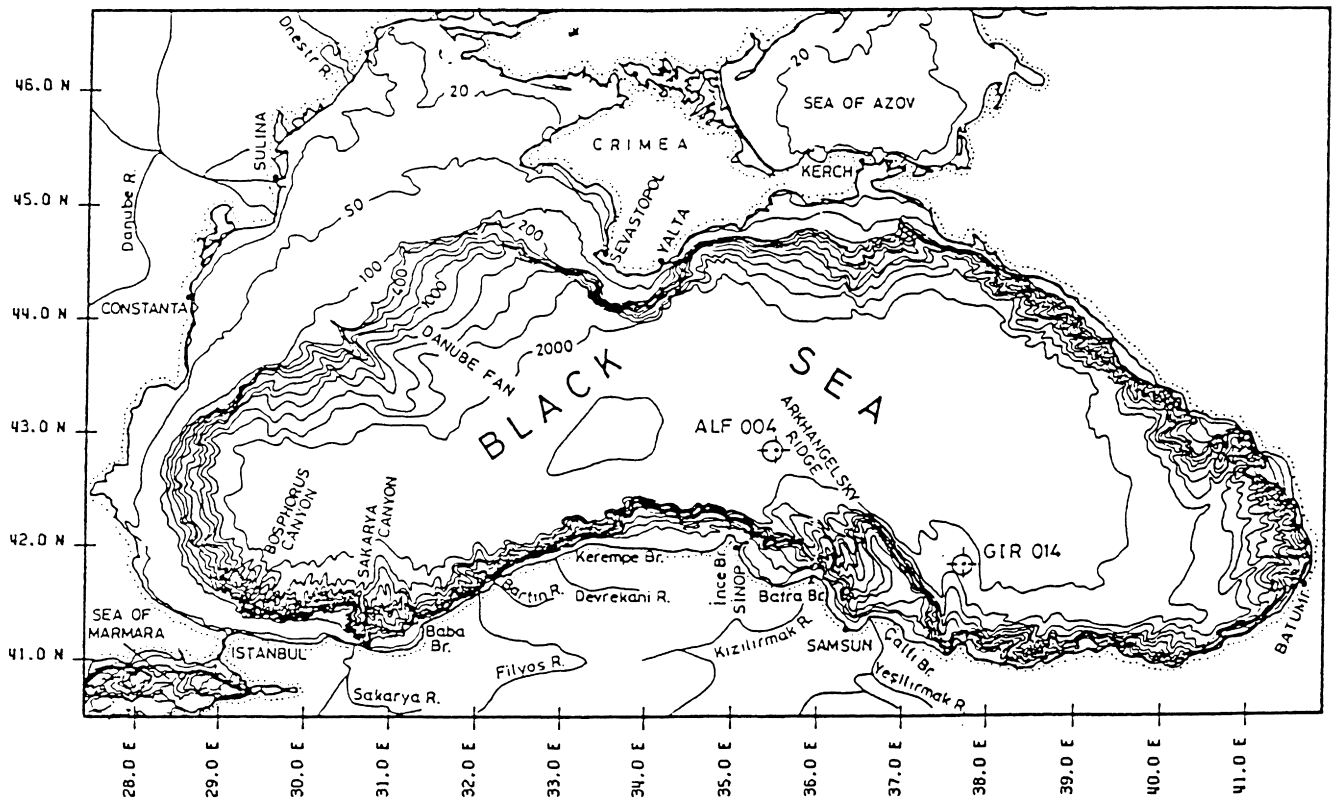

Fig. 2. Location of cores ALF-004 and GIR-014 in the Black Sea.

anoxia, aided by the decay of terrigeneous vegetation covered by the expanding sea, coincided with the deposition of sapropel–varve couples [20].

There is discussion of the exact rates of sedimentation in the Black Sea [21,22], but the processes which have just been adumbrated clearly led to a much greater organic content in Unit 2, the only Unit to be comprised of sapropels, than had existed in Unit 3. Unit 2 is surmounted firstly by a Transition Zone and then by Unit 1 (Fig. 1). There has been no deposition of sapropels since the Transition Zone and Unit 1 is formed by annual depositions of coccolith–varve couples interspersed with turbidite layers which have continued until the present day. If one assumes that all coccolith–varve couples, all sapropel–varve couples and all Turbidite layers were each deposited over the course of a year, then counting of the layers in one of the cores we have examined shows Units 1 and 2 to have been deposited over periods of about 1700 and 3800 years, respectively, values which are reasonably consistent with the durations of Units 1 and 2 previous workers have derived from the ^{14}C dating of similar cores [21,23,24]. Varve counting indicates the duration of the Transition Zone to have been shorter in the cores worked in the present studies than in those examined by previous investigators. Recent workers have ascribed the relative shortness of the durations obtained from varve counting compared with the durations derived from ^{14}C dating (apparently not true of our cores, though we have yet to obtain precise ^{14}C dates) to the absence of annual deposition in years when there was no phytoplankton bloom [21,24]. Nevertheless, the continuing sequence of annual couples interspersed with Turbidite layers forms a time-series, several thousand years in extent, which in principle contains the relationship between climate, oceanology and yearly production in the Black Sea. There has been little alteration in the composition of the turbidites in Units 2 and 1 and, although there has been a change in the rates of sedimentation in the Black Sea (Fig. 1), the reason for the change from sapropel–varve to coccolith–varve couples is not obvious. Throughout the deposition of Unit 1 until now, the Black Sea has consisted of two-layers, an upper, brackish, oxic layer and a deeper, saline, anoxic layer originating from the Mediterranean and it has been postulated that the change to the growth and deposition of coccoliths became possible and was occasioned by the increase in the salinity of the upper waters [25,26]. Today, coccolith blooms have been observed to be triggered by the input of wind-borne dust from North Africa [27] and it is possible that the change from Unit 2 to Unit 1 was accompanied by changes in the air flows over the Black Sea.

Summarising, the sapropels present in Unit 2, and only in Unit 2, were deposited but a few thousand years ago and are now less than 400 cm below the bed of the Black Sea. There is no evidence of major subsidence or uprising since

the sapropels were deposited. The sapropels will have experienced diagenesis, which could be continuing, but not catagenesis.

3. Methodology

3.1. The sapropels

Deep-sea gravity cores enclosed in plastic pipes, stored on board ship at room temperature, were inspected and two, in which the sediments were in good condition, were selected for study. These cores, termed ALF004 and GIR014, from the southern Black Sea were obtained at 42° 51′ 25″ N, 35° 56′ 23″ E and 41° 52′ 25″ N, 37° 44′ 05″ E (Lat. and Long.), respectively. Sapropels were sub-sampled from Unit 2 which was positioned normally in core ALF004, but was much nearer the sea-floor in core GIR014; presumably there was either an absence of deposition or else erosion of Unit 1, the Transition Layer and the top of Unit 2 had occurred. The sapropels were dried sufficiently carefully to retain a coherent sample with an undisturbed microscopic structure and stored under gentle refrigeration till needed for examination.

Total carbonate compositions were determined by the gasometric method [28] following treatment of ground, dry samples with dilute (10%) hydrochloric acid. Analar calcium carbonate was used as a standard. Total carbon, hydrogen and nitrogen contents were determined using a CHN analyser, acetanilide being used for calibration. The organic carbon contents of the samples were determined on a dry mass basis from the differences between the total carbon and the inorganic content calculated from the carbonate content.

3.2. Petrographic fluorescence

Petrographic briquettes were prepared from carefully dried samples of sapropel embedded in cold-setting epofix resin and then polished either parallel to or perpendicular to the axis of the gravity core. Polished specimens were initially studied and photographed by reflected light microscopy using a 32 × or a 50 × oil immersion objective ($n = 1.518$), a high pressure mercury lamp, a BG 38 and two BG12 filters and a K510 barrier filter to aid identification of the liptinite macerals. Subsequently, the fluorescence emitted by the polished liptinite macerals was observed through a computerised microscope using a high pressure 100 W mercury light source, BG 38 and BG3 filters to enhance the contrast of the morphology, a K460 barrier (cut off) filter and a 125 × oil immersion objective. Spectral intensities between 460 and 700 nm were measured, stored in an attached computer system and printed. Relative intensities were generated from the corrected intensities. The underlying principles, the basic calibration techniques and the applications of fluorescence measurements to geological samples are documented in Refs. [29–34].

3.3. Fluorescence of powders

Sub-samples of sapropels were demineralised by digestion for 48 h at 60°C in a 1:1 by volume mixture of HCl and HF, the acids being replenished after 24 h. The residues were washed until free of acid and dried at 60°C under vacuum. These dried, mineral-free sapropels were crushed by hand to a diameter of <1 μm and suspended in distilled water. The fluorescence of the suspensions was recorded on a spectrofluorometer, correction being achieved in accordance with the instrument instructions [35]. The excitation and emission 'bandpass' was 5 nm.

3.4. Py.-g.c./m.s. analyses

The demineralised sapropels were pyrolysed in an integrated system comprising a CDC pyroprobe heated-filament pyrolyser, a gas chromatograph and an ion-trap mass spectrometer. The experimental procedure was similar to that used for the structural analysis of recent sediments [36], a pyrolysis temperature of 700°C being held for 10 s, the interface to the gas chromatograph being maintained at 250°C, the carrier gas flowing at 2 ml/min and a split ratio of 1:30 being utilised. Five samples were pyrolysed in the presence of tetramethyl ammonium hydroxide [37].

3.5. Nuclear magnetic resonance

The ^{13}C NMR spectra of demineralised sapropel samples were obtained by the cross polarisation, magic angle spinning technique at 25 MHz with a contact time of 1 ms and a delay of 1.5 s between successive contacts. 250 mg of sample powdered to less than 250 μm diameter was packed inside a 7 mm diameter zirconia rotor. Typically over 1000 scans were accumulated and spectra were processed using a line broadening factor of 30 Hz.

3.6. Removal of pyrite

All kerogens were initially washed with 0.1 M HCl to ensure that, among others, calcium minerals had been removed which could absorb some of the H_2S produced during high pressure t.p.r. Pyrite was removed by treating with $CrCl_2$ according to the method of Acholla and Orr [38]. Acidic $Cr(II)Cl_2$ was prepared by passing a 2 M $CrCl_3$/0.5 M HCl solution through an amalgamated Zn "Jones reduction" column. The $CrCl_2$ solution and concentrated HCl (2:1 v/v) were added dropwise to an ethanol/kerogen slurry purged with nitrogen. The mixture was refluxed for 2 h under nitrogen which was bubbled through a 3% $AgNO_3$ trap. After cooling, the contents of the flask were filtered. The residue was rinsed with CH_3OH/CH_2Cl_2 and dried in a vacuum oven at 60°C.

3.7. Temperature programmed reduction

The operation of the high pressure t.p.r. system has been described elsewhere [39]. Typically, 50 mg of finely ground,

Table 1
Composition of Unit 2

Core	$CaCO_3$ (wt%)	C_{org} (wt%)	Total H (wt%)	Total H (wt%)	H/C[a]	H/C[b]	O/C[c]
ALF-004							
Sapropel	7.6	12.7	0.9	2.35	1.3–1.5	1.4–1.5	0.15–0.25
Turbidite	13.6	0.74	0.05	0.76	–	–	–
GIR-014							
Sapropel	6.75	7.92	0.51	1.82	1.1–1.3	1.5	0.13–0.17
Turbidite	10.64	1.35	0.1	0.85	–	–	–
Type 1 kerogen oil shale	–	–	–	–	1.6	1.5	0.15–0.22

[a] Elemental analysis.
[b] Calculated from the ^{13}C NMR spectra of the organic material assuming the average aliphatic structure was CH_2.
[c] Calculated from the ^{13}C NMR spectra of the organic material assuming the presence of phenols and aromatic OCH_3 ethers but no other aromatic ethers or heterocycles (whose presence would lower the ratio). The lower value is obtained if aliphatic ethers but not alcohols were present; the higher value assumes the presence of alcohols but not aliphatic ethers.

pyrite-free sapropel was diluted in a 1:10 w/w mixture with acid-washed sand (75–250 μm) to increase the voidage in the fixed bed. The samples were heated from ambient to 600°C at 5°C/min with a hydrogen flow rate of 5 $dm^3\ min^{-1}$ (measured under ambient conditions and corresponding to a gas velocity of around 0.5 ms^{-1} in the reactor). Liquid products were collected in an ice-cold trap and were recovered in dichloromethane at the end of each run. The hydrogen sulphide evolved from the reactor was detected by a quadrupole mass spectrometer.

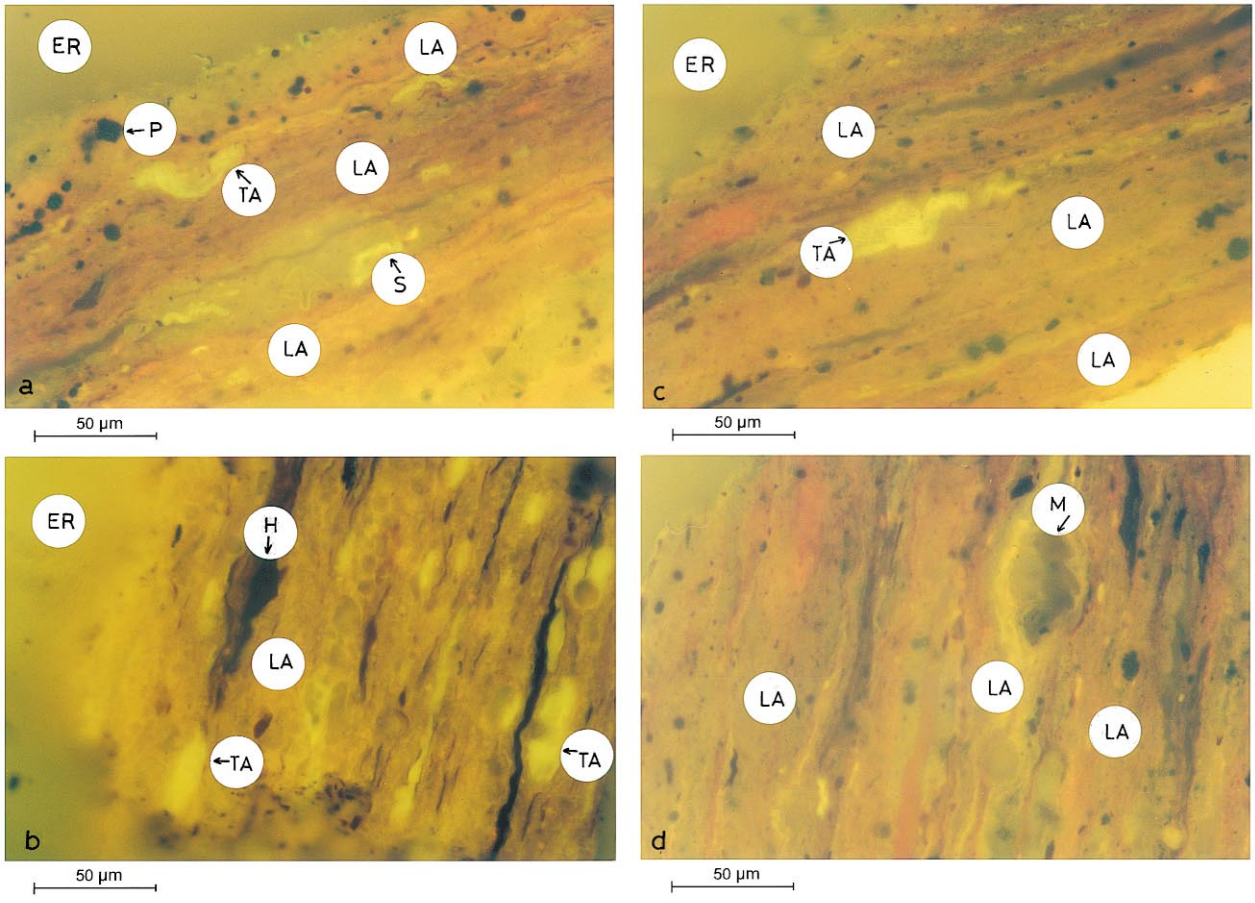

Fig. 3. Fluorescence microscopy of the sapropels showing their petrography in oil immersion. (a), (c) and (d) Core ALF-004 (337 cm + 2195 m depth). (b) Core GIR-014 (18 cm + 1945 m depth). Depths are given as depth in sediment (cm) + depth of water column (m). ER = Epofix resin; H = Detrital huminite; LA = Lamalginite (Alginite B); M = Mineral matter; P = Pyrite; S = Sporinite; TA = Telalginite (Alginite A).

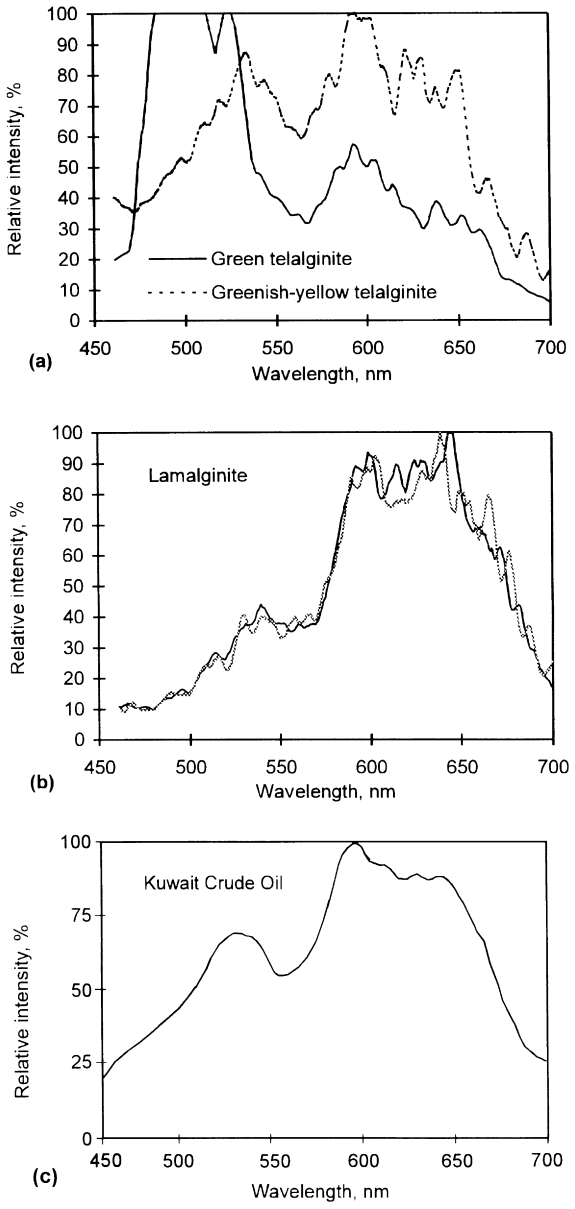

Fig. 4. Emission spectra from polished surfaces of: (a) sapropel–varve couples; (b) a Type 1 kerogen oil shale; and (c) Kuwait crude oil (Excitation by mercury light).

4. Results and discussion

4.1. The composition of Unit 2 in the gravity cores

Unit 2 appeared similar in both cores even though Unit 1 was missing from core GIR-014. Table 1 lists the percentages of carbonate and organic carbon present in the Unit as well as the elemental analysis of the organic matter. Reflectance microscopy and Table 1 indicate that Unit 2 in both ALF-004 and GIR-014 cores conforms to the characteristics recorded by previous workers. In particular, Table 1 confirms the relatively high organic content of the sapropels and, their atomic H/C ratios being 1.1–1.5, the probability, consistent with previous work [14–16], that much of their organic composition is aliphatic. The carbonate content of the sapropels is naturally lower than that of the turbidites.

4.2. Petrography

Transmission microscopy (smear slides) has identified numerous fossil organisms, often diatoms, in the sediments below the Black Sea [40]. We have observed many such fossils in the sapropels by scanning electron microscopy. Furthermore, as previous workers have found [41], scanning electron microscopy revealed the sapropels to comprise layers of microlamellae. This is confirmed and extended by their petrography. Since the sapropels were muds of soft particles, their examination by reflected light was difficult but carefully dried sapropels fluoresced brightly and predominantly green. When viewed ‘edge-on’ (parallel to the bedding plane, not shown in the photographs) the annual sapropel–varve couples were seen as parallel, fluorescing organic sheets which could be counted readily. In both Black Sea cores, each sapropel–varve sheet was of the order of 50 μm thick and over several sheets the alginite layer might change in colour from yellow to green to brown. Fig. 3 shows photographs illustrating the morphologies of the liptinite macerals observed in the polished sapropel surfaces (viewed perpendicular to the bedding plane). These morphologies were very similar to those revealed in the polished surface of the Type 1 kerogen oil shale used for comparison [17]. Both the oil shale and the sapropels could be seen to consist of sheets of alginite which were relatively free of biological structure though it is possible that optical or electron microscopy might have revealed plant structure had the sheets been examined at greater resolution than we found possible. In the oil shale nomenclature of Hutton [42], we were observing lamalginite mixed with small amounts of bounded telalginite and occasional inclusions of resinite, sporinite, huminite and inertinite in a ground mass of mineral matter and, whereas the Black Sea sapropels and the Type 1 kerogen should be classified as marinites and lamosite respectively [42], their petrography was very similar.

Fig. 4 shows emission spectra from polished surfaces of the sapropel–varve couples and from the oil shale. Three distinct, major bands centred near 550 nm (green), 600 nm and 650 nm (red), were excited by mercury light though this resolution was obtained at the expense of a low signal to noise ratio. Similar bands are observed in other liptinites and Table 2 compares fluorescence from the liptinite macerals in the sapropels and the oil shale, from liptinites in subbituminous coals we have previously examined [43], and from Kuwait crude oil, whose fluorescence is typical of that of Middle East crudes. Table 2 indicates that telalginites

Table 2
Emission ratios of liptinite macerals

Sample	Geological age	Maceral	I (600/550)[a]	I (650/550)[a]
Coal: sub-bituminous	Mid-Miocene	Sporinite	2.4	3.1
		Cutinite	2.5	3.0
		Resinite	1.7	1.5
		Lamalaginite	1.8	1.6
		Telalginite	0.7	0.5
Oil shale	Jurassic–Cretaceous	Lamalginite	2.5	2.8
Kuwait crude	Not known		1.6	1.4
Sapropel (Black Sea)	Holocene	Sporinite	2.5	2.8
		Resinite	3.5	4.4
		Lamalginite	2.5	3.1
		Telalginite	1.0	1.0

[a] Average ratios of emission intensities at the stated wavelengths; excitation at 365 nm.

may often be distinguished from other liptinite macerals by the intensity of their fluorescence between 500 and 550 nm. The Table also demonstrates that despite the difference in their geological ages, the ratios of resolved red/green emission from the lamalginite and the telalginite were similar in both the Black Sea sapropels and the Type 1 kerogen oil shale.

4.3. The fluorescence of powdered sapropels

The chemistry of the impure lamalginite (marinite) comprising the sapropels can be described by starting with the interpretation of the fluorescence spectra. In fact, it is best to examine the fluorescence of suspensions of transparent particles generated after demineralisation of the sapropels since such suspensions can yield excitation as well as emission spectra. Obviously, the suspensions consist of dispersed organic matter and in this terminology [44], the impure lamalginite would be classified as relatively structureless palynodebris deriving from algae, principally micro-algae. Fig. 5a–e illustrate the fluorescence of aqueous suspensions of powdered sapropels. These corrected spectra extend only to 600 nm and, since they were obtained from the complete sapropel, they derive from the average organic structure of the impure marinite. Fig. 5a shows the fluorescence emitted by sapropels excited by 365 nm light. This wavelength is within the range generated by the mercury lamp exciting fluorescence in the petrographic studies and the similarity of the emission spectra in Figs. 4 and 5a in the range 450–600 nm, in particular the significant peak close to 550 nm, confirms the quantitative reliability of the petrographic spectra in this region.

Fig. 5b shows a typical sapropel emission spectrum generated by excitation at 230 nm. Besides the emission near 550 nm, the spectrum shows pronounced maxima at 300–310, 340–350 and ~400 nm. Excitation spectra corresponding to the maximum at 300–310 nm (Fig. 5c) show peaks near 230 and 270 nm, consistent with the presence of substituted benzenes, in particular, perhaps, of substituted phenols. Alkyl benzenes and alkyl phenols have frequently been found in liptinite [16,49], and will be identified in the sapropels by Py.-g.c./m.s. Excitation spectra of the 340–350 nm emission maximum (Fig. 5c) exhibit peaks near 230 and 270 nm (broad) suggesting the 340–350 nm emission to arise from naphthalene structures and substituted naphthalenes will indeed be shown to be amongst the products generated by Py.-g.c./m.s. of the sapropels.

The emission at ~400 nm is associated with humic acids. Fig. 5d shows this emission to correspond to excitation near 320 nm and with poorly resolved, weak maxima near 240, 270 and 310 nm. Polynuclear aromatic hydrocarbons which might have accounted for emission ~400 nm were not observed amongst the products of Py.-g.c./m.s. and, accordingly, the emission is ascribed to the presence of either, or probably both, substituted naphthols and hydroxylated benzoic acids. Examples of both these structures are known which fluoresce at the appropriate wavelengths.

The emission near 550 nm has been seen to occur from many liptinite macerals, it dominates the emission from telalginites (Table 2 and Fig. 4) and is often generated by fossil fuels (such as the Kuwait crude-oil and the Type 1 kerogen studied here, Fig. 5f). Accordingly, one suggests that the 550 nm emission maximum observed in sea water and monitored by satellites should be associated with the presence of algae. It has been ascribed to flavin structures [45]. Flavins give characteristic products in Py.-g.c./m.s., none of which were observed in the sapropels. The 550 nm emission from sapropels corresponded to a series of approximately equally intense excitation maxima at around 250, 417, 435, 490, 510 and 540 nm and it is suggested that the fluorescence may have arisen from unsaturated hydrocarbons (carotenoids) known to be present in micro-algae [46,47].

In keeping with the discussion in later sections, we attribute the petrographic fluorescence maxima of the sapropels

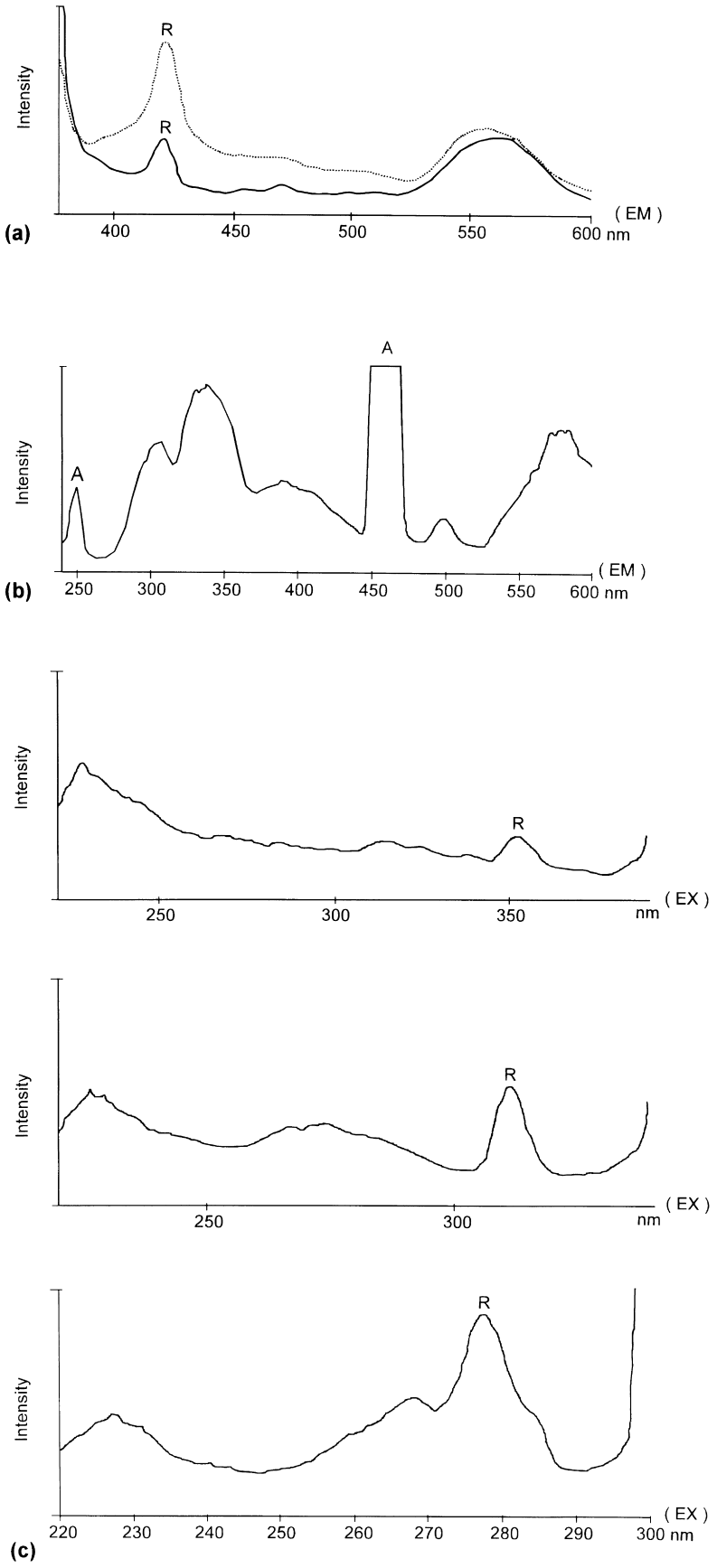
R
R
Intensity
(EM)
400
450
500
550
600 nm
(a)
A
A
Intensity
(EM)
250
300
350
400
450
500
550
600 nm
(b)
Intensity
R
(EX)
250
300
350
nm
Intensity
R
(EX)
250
300
nm
Intensity
R
(EX)
220
230
240
250
260
270
280
290
300 nm
(c)

Fig. 5.

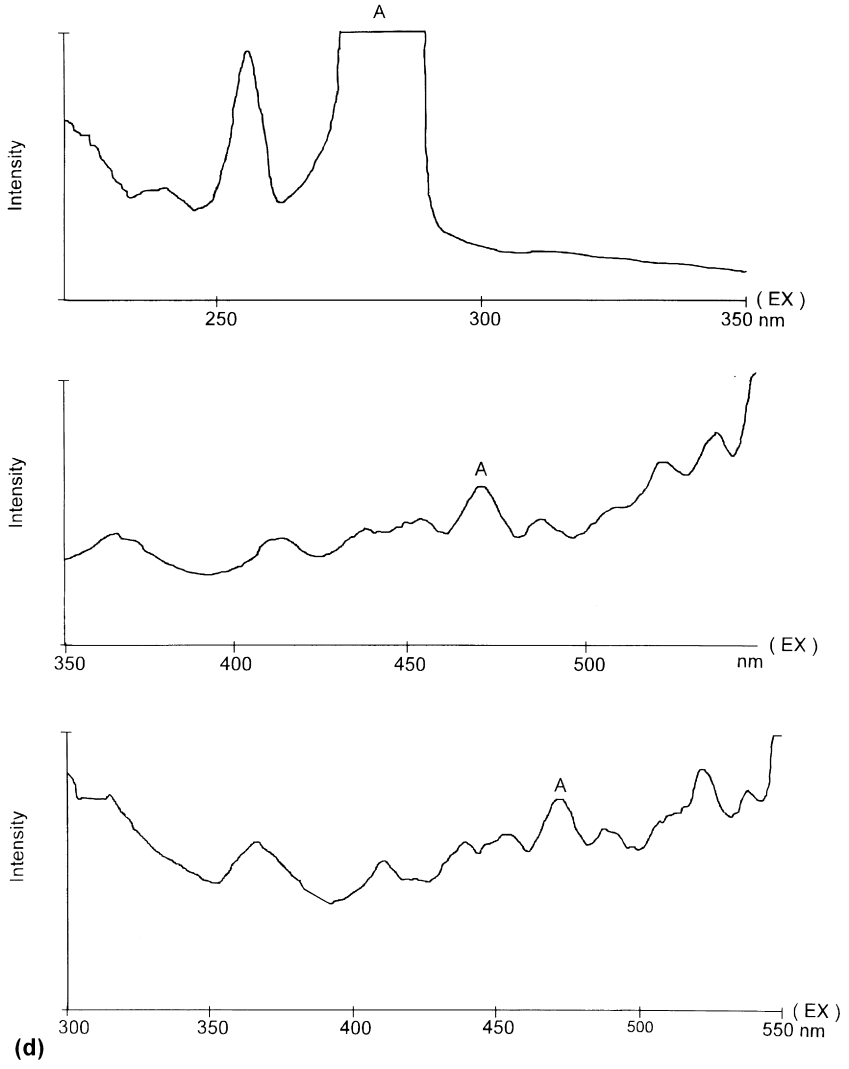

Fig. 5. (*continued*)

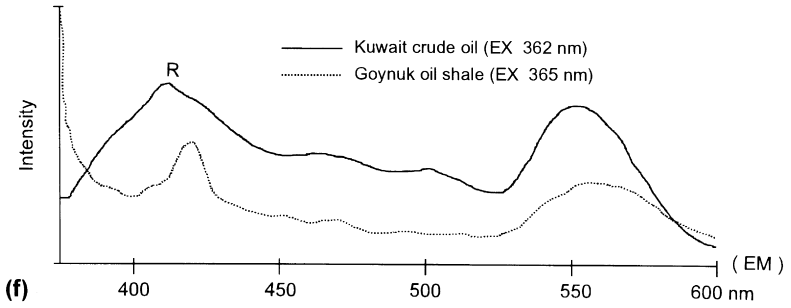

Fig. 5. Corrected spectra of aqueous suspensions of demineralised sapropel powders. (a) Emission spectra (Ex 365 nm): solid line, core GIR-014; dashed line, core ALF-004. (b) Emission spectrum (Ex 230 nm): core GIR-014. (c) Excitation spectra (Em 307, 350 and 400 nm): core GIR-014. (d) Excitation spectra (Em 557 and 560 nm): top and middle core GIR-014; bottom Type 1 oil shale. (e) Excitation spectra (Em 600 nm—top; 650 nm—bottom); core GIR-014. (f) Emission spectra (Ex 365 and 362 nm); Kuwait crude oil and Type 1 oil shale (Goynuk). Ex = Excitation; Em = emission; peaks marked A are artefacts; peaks marked R are due to Raman scattering by water.

at 600 and 650 nm to phaeopigments (or chlorophylls) which fluoresce at these wavelengths, this being consistent with the liptinite macerals originating from the outer cell membranes of vegetation. The association of emission at 540 nm with the fluorescence at 600 and 650 nm might then be explained by the known involvement of carotenes with photosynthesis in the chloroplasts. Fig. 5e shows corrected excitation spectra from sapropel suspensions corresponding to emission at 600 and 650 nm. The most intense peaks in the excitation spectra are those in the ultraviolet at 220–230 and 270–290 nm. These peaks were not observed in the fluorescence of solutions of chlorophyll or phaeopigments and it is speculated that these excitation maxima are due to alkyl aromatics, which transfer light energy to the residues of the algal photosystem remaining in the sapropels. Such alkyl aromatics could derive from aromatic carotenes or the aromatic residues of the proteins supporting the algal photosystem.

4.4. ^{14}C NMR spectroscopy

Fluorescence spectroscopy is a sensitive technique and the compounds discussed in the previous section were undoubtedly present in the sapropels only in low concentrations. ^{13}C NMR spectrometry was used to determine the average organic composition of the impure lamalginites (marinites) which petrography has shown to comprise the sapropels.

Fig. 6 shows typical sapropel spectra, together with the spectrum from the Type 1 kerogen oil shale. The two materials are clearly very similar in structure and generated spectra similar to those of other alginites [48]. Superficially similar spectra are also generated by cutinites [48], and even by Carboniferous sporinites [49,50], where prolonged catagenesis appears to have made little qualitative difference to the liptinite structure. All these liptinite spectra are dominated by a relatively sharp resonance near 30 ppm, characteristic of long alkyl chains (carbon atoms gamma and further from a terminal methyl), but differ in their aromaticity and in the details of their aliphatic structures. In Fig. 6, the dominant resonance at 30 ppm is broadened by overlap with peaks from alkyl groups bonded directly to aromatic rings and noticeable as shoulders in the regions of 18–21

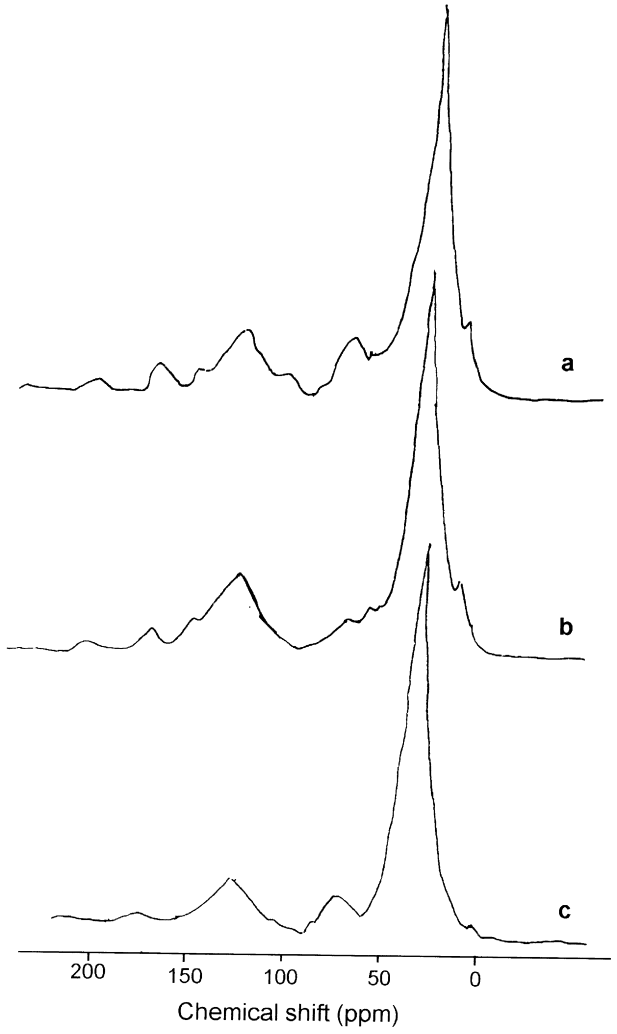

Fig. 6. CP/MAS ^{13}C NMR spectra: (a) sapropel from ALF-004; (b) sapropel from GIR-014; (c) Type 1 kerogen oil shale.

Table 3
Summary of ^{13}C NMR data

Sample	Depth down core (cm)	f_a[a]	COOH[b]	CO[b]	CH_nO	ArC–O/ArC–H	CH_2/CH_3[c]
GIR-014	15	0.25	0.8	0.5	2.5	0.4	5.3
ALF-004	362	0.20	0.7	0.3	2.5	0.5	4.6
ALF-004	365	0.20	0.75	0.4	1.7	0.4	4.8
ALF-004	372	0.19	0.6	0.1	2.9	0.4	5.0
ALF-004	380	0.21	0.6	0.4	2.1	0.5	5.6
Oil shale	(top)	0.15	–	–	–	–	6.6
Oil shale	(bottom)	0.15	–	–	–	–	6.9

[a] Fraction of aromatic carbon of the total carbon (excludes sp^2 carbon present as C=O).
[b] Ratio to the number of terminal methyl groups.
[c] Ratio of the height of the major methylene peak near 30 ppm to the height of the terminal methyl peak close to 15 ppm.

and 39 ppm. (These interpretations are based on those of Snape et al. Ref. [51], but see also Ref. [49]). The methyl groups that terminate alkyl chains give the small but sharp peak near 15 ppm. There is defined absorption at 62 and 73 ppm which may be ascribed to carbon atoms bonded to ether linkages. Cellulose absorbs at both these chemical shifts and it is tempting to suggest these peaks derive from cellulose that has escaped diagenesis, but cellulose also gives additional peaks at 89 and 105 ppm which are not observable in the present spectra.

The aromatic carbon peaks occurring between 100 and 160 ppm may be resolved into carbon atoms bonded to hydrogen, carbon and oxygen atoms, the latter being particularly clearly resolved. Aromaticities, f_a, are all about 0.2, although due to underestimation by Cross Polarisation, these are probably closer to 0.3 as reported elsewhere for the Type 1 kerogen [52]. Weak absorption by carboxyl groups (close to 170 ppm) and carbonyl groups (near to 210 ppm) is apparent. Table 3 compares the bulk structural parameters for the five sapropel samples and the two samples of the Type 1 kerogen oil shale. The bulk organic structure of the sapropels is clearly very similar to that of the oil shale, although the sapropels may be marginally more aromatic and possess a slightly smaller average chain length. The quantitative similarity of the ^{13}C NMR spectra of the sapropels and the oil shales extends to the estimates of their elemental H/C and O/C ratios listed in Table 1. The differences between the GIR-014 and the ALF-004 sapropel spectra and also between the spectra of ALF sapropels obtained at different depths appear to be within the experimental error of the technique. Thus, the results suggest the sapropels to possess a similar organic composition throughout Unit 2.

Although the aromic H/C ratios determined by elemental analysis suggest the sapropels to be Type 1-2 kerogens, the ratios estimated from ^{13}C NMR (Table 1), together with the low aromaticities, indicate that their bulk compositions must resemble those in the Type 1 kerogen oil shale very closely.

4.5. Identification of organic sulphur forms by high pressure t.p.r.

We have found 0–2 wt% of sulphur in dried, mineral-free samples of the sapropels. The presence of sulphur and pyrite is often noted as a characteristic of marine deposition and sulphur groups can be important in the formation and thermal decomposition of kerogen and therefore in the generation of crude oil [53,54]. In the absence of iron compounds, inorganic sulphur nucleophiles combine with unsaturated lipids and alkenes and perhaps carbohydrates to form S–S and C–S cross-links in the resulting kerogen but the relative weakness of these bonds permits high-sulphur kerogens to generate petroleum at lower temperatures than low sulphur kerogens [55–57].

In t.p.r. under high pressures of hydrogen, over 80% of the organic sulphur is reduced to hydrogen sulphide with the remainder being reduced to tar, and, in consequence, the resolution of the organic sulphur speciation is superior to that of photoelectron spectroscopy (XPS) and X-ray absorption near edge structures (XANES) [58]. Fig. 7 shows the hydrogen sulphide evolution profile from sapropel GIR-014. Of that evolved, 80% occurred between 200 and 380°C, with a dominant peak at a little below 300°C. This is consistent with a mixture of aliphatic and aromatic sulphides being the dominant form, which can be assumed to have been formed already in the early stages of sedimentation in the anoxic Black Sea environment by the combination of inorganic sulphur nucleophiles with unsaturated lipids or alkenes [58,59]. Sulphides yield hydrogen sulphide on pyrolysis and are not observed by Py.-g.c./m.s. The absence of distinct peaks below 250°C suggests that di/polysulphides and thiols are present in relatively low concentrations in relation to the sulphides. The peak centred at 400°C (Fig. 7) can probably be attributed to single ring thiophenes formed by diagenesis [53,54,58,59]. The observation of thiophenes under these conditions confirms the reality of their presence when observed by Py.-g.c./m.s. [36]. Other Black Sea sapropels gave similar t.p.r. profiles consistent with all the samples having similar maturity. The t.p.r. of the Type 1 kerogen oil shale with which the sapropels are being compared has

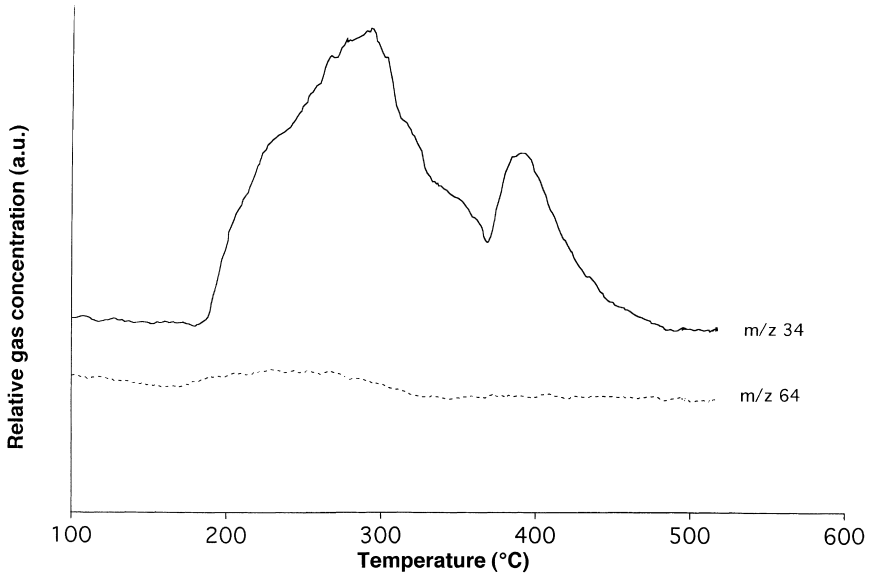

Fig. 7. High pressure temperature programmed reduction evolution profile for GIR-014.

already been published [59]. Compared with Fig. 7 the thiophene peak from the oil shale was much less well resolved, but the major peak was slightly in excess of 300°C, consistent with mono-sulphides being the dominant species.

The t.p.r. profiles suggest the samples examined from the GIR-014 core to resemble the lower section, approximately 100 m deep, of the immature Peru margin sediments, which, in terms of sulphur geochemistry, is thought to be a modern analogue of the Miocene Monterey Fm sediment [60]. However, for samples taken from the surface of this sediment di/polysulphides were the dominant sulphur species [59]. This difference with the Black Sea sediments could arise either from the greater availability of reduced sulphur in the Peru margin compared to the Black Sea or from the greater rapidity of the transformation between di/poly and mono-sulphides in the Black Sea environment.

4.6. Pyrolysis-gas chromatography/mass spectrometry

4.6.1. Yields and reproducibility

Petrography has shown the Black Sea sapropels to consist of sheets of impure lamalginite (marinite) whose average composition has been revealed by ^{13}C NMR spectroscopy (Table 3). Complementary characterisation of the major individual structures present in the sheets can be generated by Py.-g.c./m.s. which was applied to a sequence of five sub-samples of sapropel from the GIR-014 core. These sub-samples gave similar results and Table 4 lists 46 compounds released by pyrolysis, each of which were at least partially identified. The relative intensities of each compound have been expressed as percentages of the total area occupied in the gas chromatogram.

One sapropel sub-sample was pyrolysed and analysed three times. The repeatability was good inasmuch as the standard deviations of an individual result generally varied between only 1 and 6% of the corresponding mean, though there were some exceptions (Table 4). There was little systematic change in the composition of the organic material with the depth of the sapropel within the core. When the five GIR-014 sapropel sub-samples from different depths were compared, of the 46 compounds listed in Table 4, 17 gave means and standard deviations which were virtually identical with those obtained from repeated measurements of the uppermost sapropel. These 17 compounds (table footnote “d”) generally possessed rather stable structures which resisted pyrolysis and perhaps, therefore, diagenesis. Other compounds, more susceptible to pyrolysis, did give increased standard deviations when the five sapropel sub-samples from different depths were compared. Thus, alkene to alkane ratios had larger variances when five sapropels were investigated than when measurements were repeated on a single sapropel, a clear indication that the effects of pyrolysis changed from sub-sample to sub-sample.

When a sapropel is heated on a hot wire secondary, retrogressive reactions are minimised by rapid heating (100,000°C/s) in a flow of the helium carrier gas [61]. Nevertheless, both we and van de Meent et al. [16] observed a 50% yield of unresolvable tarry matter from Py.-g.c./m.s. assays of sapropels. It is clear that the Black Sea sapropels possessed a matrix giving significant yields of involatile products on pyrolysis.

4.6.2. The nature and origin of the pyrolysis products

The material generated by Py.-g.c./m.s. consisted of alkanes (16%), alkenes (28%), alkyl benzenes (including unsaturated alkyls) (35%), alkylated naphthalenes and some phenols (Table 4). It has already been noted that the fluorescence of the sapropels was consistent with the presence of alkylated benzenes, phenols and naphthalenes.

Table 4
Compounds observed by Py.-g.c./m.s.

Compound/mass	Scan	Mean[a]	%SD1[b]	%SD2[c]
Toluene + Me-thiophene	139	9.1	2	6
m/p xylene	228	2.9	4	20
Styrene + *o*-xylene	254	5.1	5	6[d]
2-Me-cyclopenteneone	267	1.65	3	4
Me-ethylthiophene	351	3.5	10	9[d]
+ C_3 benzene phenol	382	2.2	20	17[d]
C_3-benzene + indane	402	5.4	5	7[d]
Decane	416	1.2	8	12
C_3-benzene	444	0.9	5	7[d]
124, 117, 110, 109	467	1.2	4	17
Indene	483	1.3	5	15
o-Me phenol	504	1.5	5	6[d]
Ph-propanone	521	0.95	1	11
Undecene	574	2.9	11	11[d]
Undecane	589	1.5	9	10[d]
130, 115	663	0.65	15	18[d]
C_4-benzene	668	2.5	5	17
130, 115	677	1.1	6	7[d]
Dodecene	750	2.8	6	11
Dodecane	766	1.55	3	7
Dimethyl indene	848	0.55	3	11
133, 132, 104	888	1.0	3	20
2-Me naphthalene	917	0.9	8	8[d]
Tridecene	922	4.2	4	12
Tridecane	936	2.3	6	7[d]
Tetradecene	1086	2.7	8	6[d]
Tetradecane	1099	2.6	10	25
di-Me-naphthalene	1116	0.6	1	24
di-Me-naphthalene	1122	0.75	4	12
Octylbenzene	1197	1.0	2	29
Pentadecene	1242	5.12	4	13
Pentadecane	1253	3.5	6	29
208, 138, 125	1329	1.6	1	66
Hexadecene	1389	2.9	6	11
Hexadecane	1400	1.9	6	15
Decylbenzene	1500	0.7	15	19
Heptadecene	1530	4.1	6	16
Heptadecane	1540	1.9	3	6[d]
212, 197, 155	1558	1.1	9	14
266, 125, 111	1576	2.3	2	2.5[d]
Octadecene	1663	1.4	4	8
Octadecane	1672	1.45	3	8
270, 185, 143	1687	0.4	32	50
272, 229, 149	1692	1.35	16	22
272, 229, 119	1765	1.0	4	13
Nonadecene	1791	1.3	8	9[d]

[a] Means are expressed as a percentage of the total peak area and are calculated from analyses of five sapropels.
[b] SD1 = standard deviation calculated from three repeated experiments on the same sample as a percentage of the mean.
[c] SD2 = Standard deviation calculated from five sapropels as a percentage of the mean.
[d] SD2 values were virtually identical with the SD1 of the uppermost sapropel.

Consistent with the investigation by t.p.r., alkyl thiophenes were also observed by Py.-g.c./m.s. and the presence of dialkyl substituents may indicate that these thiophenes were formed from straight chain aliphatics [62].

Not only has petrography shown the sapropels to be impure lamalginites (marinites), there was only a small amount of liptinite which could be ascribed to terrigeneous spores and cuticles. Consistent with petrography, Table 4 records no phenols characteristic of lignin monomers. The compounds listed in Table 4 therefore had an aquatic, probably a marine origin. Few of the compounds obtained by the pyrolyses of the sapropels can be recognised as markers of either carbohydrates or of protein. Whereas the observation of methyl derivatives of 3- and 4-hydroxybenzoic acids, phenol, 4 methyl phenol and di- and tri-methyl phenols when pyrolysis was repeated in the presence of tetramethyl ammonium hydroxide (TMAH), was clearly consistent with the original identification of the parent compounds (Table 4), the absence of methylated markers of glucose and the presence of only low concentrations of methylated markers of cellulose (both easily recognised in the pyrolysis of younger material [37]) confirmed the removal of carbohydrates during diagenesis either in the water column or by bacterial action in the sediment.

The distributions of alkanes and alkyl benzenes obtained by pyrolysis (Fig. 8) remained virtually unchanged whether or not the sapropels were pre-extracted with chloroform or dichloromethane. The relatively low molecular mass compounds recorded in Table 4 therefore derived mainly from kerogen, since little additional solvent extractable material (bitumen 2) was obtained after demineralisation. All the evidence from Py.-g.c./m.s. confirms the conclusion from ^{13}C NMR that the chemical structure of the sapropels bears no simple relationship to that of newly sedimented material, but is broadly similar to that of Type 1 kerogen. Py.-g.c./m.s. of the Type 1 kerogen referred to for comparison in Table 1 did indeed give very similar results (Fig. 10) to those of the sapropels.

4.6.3. Alkanes

The greatest concentrations of *n*-alkanes generated by pyrolysis occurred around C_{15} (Fig. 8). This is consistent with a crude comparison of the estimated gamma CH_2/CH_3 ratios obtained by ^{13}C NMR (Table 3) which range from 4.6 to 5.6, that is, from 6.6 to 7.6 when alpha and beta CH_2 are included. Interestingly, *n*-alkanes observed by g.c./m.s. in the bitumens had their highest concentrations at C_{25}. Although this is a slightly lower carbon number than previously observed by the gc/ms of bitumen from Black Sea sediments [10,11], it suggests there was an allochthanous input to the relatively small amount of bitumen. Indeed, Simoneit found bitumen from Pleistocene and Pliocene Black Sea sediments to have an allochthanous origin [10,11] and Love et al. [63] have identified higher plant input into the Type 1 kerogen.

Alkanes and alkenes observed in Py.-g.c./m.s. may either have occurred as such in the sapropels or may have been formed by the pyrolysis of lipids. Sun and Wakeham [22], found it sufficient to postulate single pools of labile and refractory lipids to model diagenesis in the first 50 years of anoxic Black Sea sediments and probably the labile lipids

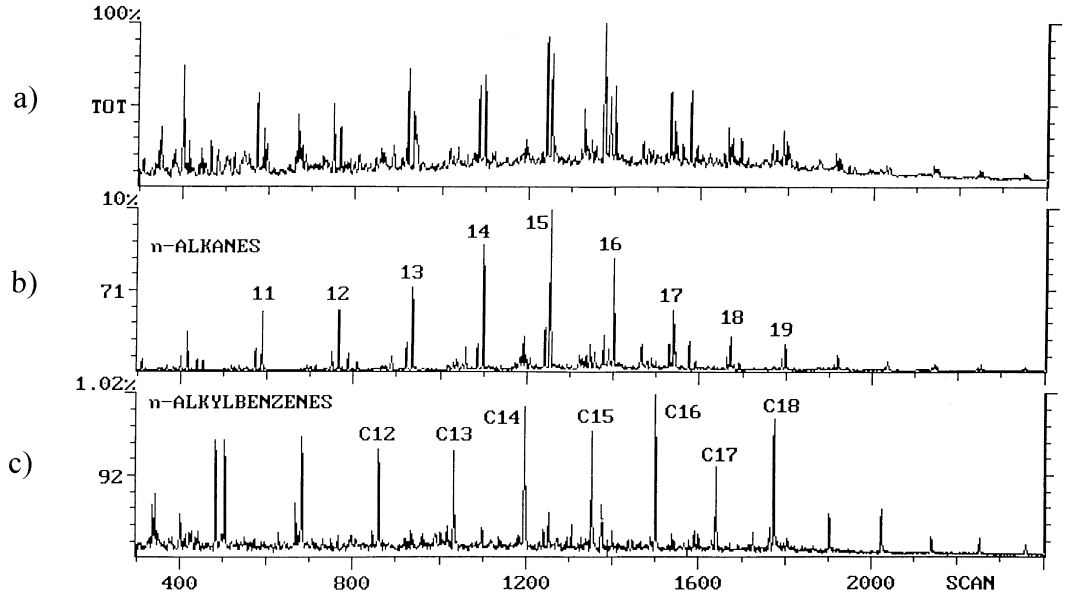

Fig. 8. Py.-g.c./m.s. of Black Sea sapropels: (a) total ion current; (b) obtained by monitoring *m/z* = 71; (c) obtained by monitoring m/z = 92.

can be assumed to be fatty acids which are frequently found in sediments. That fatty acids in the sapropels indeed gave alkanes on pyrolysis was indicated by our repetition of the Py.-g.c./m.s. in the presence of TMAH. Fig. 8 shows the alkane/alkene distribution generated by normal Py.-g.c./m.s. with a maximum at nC_{15}. In the presence of TMAH the distribution of normal alkanes changed significantly and was dominated by peaks from a range of methyl esters [37], the nC_{16} methyl ester being very prominent (Fig. 9). One presumes that, in the absence of TMAH, the alkanes produced around C_{15} were derived from fatty acids originating from lipids in phytoplankton [46,64,65], and these would account for the small carboxyl peak noted in the ^{13}C NMR spectra. Py.-g.c./m.s. of pure *n*-hexadecanoic (palmitic) acid was observed to generate not only the C_{15} alkane but also several smaller alkanes all in nearly equal intensity. Previous authors have observed alkanes up to C_{30} to be generated by pyrolysis of non-hydrolysable material (termed algaenan) from the cell walls of micro-algae, particularly of fresh water microalgae

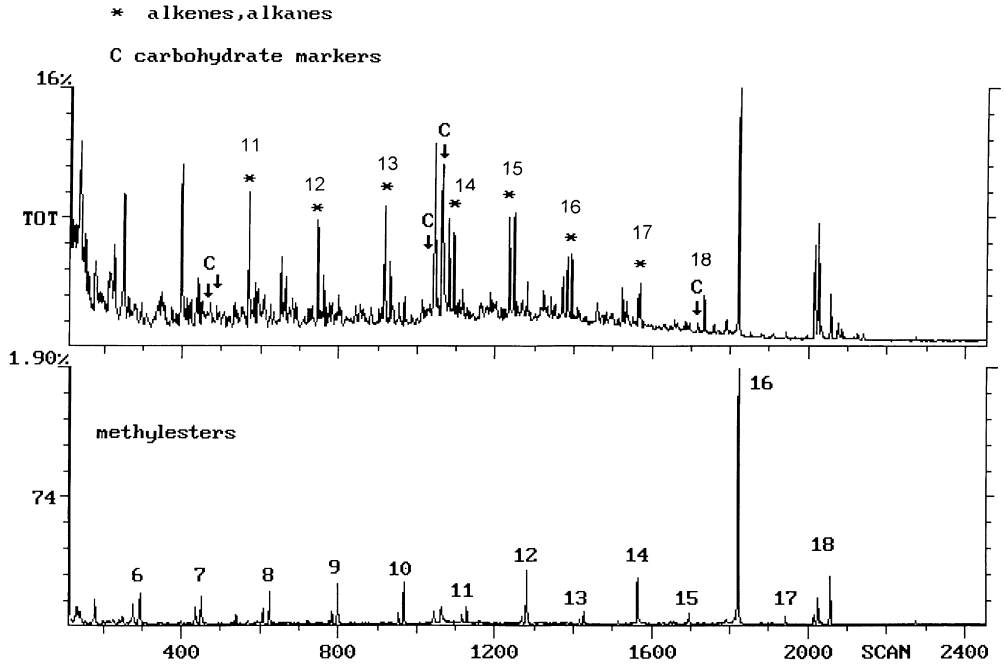

Fig. 9. Py.-g.c./m.s. in the presence of tetramethylammonium hydroxide. Top: total ion current; bottom: methyl esters visualised by monitoring *m/z* = 74.

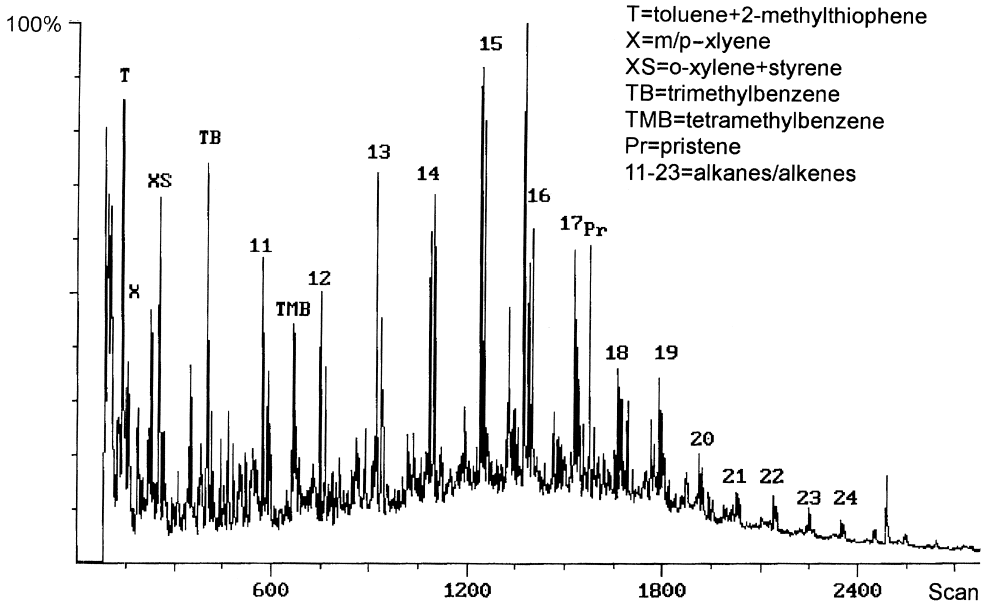

Fig. 10. Py.-g.c./m.s. (total ion current) of a Type 1 kerogen oil shale.

[66,67], though not apparently from dinoflagellates or diatoms. The material is lipoidal in that it consists of polymerised long chain esters rendered stable by ether crosslinks [67].

Flash pyrolysis of the Type 1 kerogen employed for comparison (Fig. 10) generated a multiplet of peaks around each alkane and careful inspection showed the major peaks to be, in order of elution, a diene, a monoalkene (olefin) and the alkane. A pristene peak was very prominent between the C_{17} and C_{18} alkanes. The Type 1 kerogen was lacustrine. If it is correct to suppose that sapropel formation ceased and coccoliths formed due to increasing salinity in the upper layer of the Black Sea [25,26], then, conversely, sapropels were formed in water which was less saline than the present brackish upper layer. This may explain how the Black Sea marine sapropels came to have similar structures to those found in the lacustrine oil shale.

4.7. Comparison with the results of previous authors: the structure of liptinites

4.7.1. The structure of liptinite

This section compares the chemical structures in the impure lamalginite (marinite) comprising the sapropel sheets with those structures previously found in other liptinite macerals, specifically, sporinites, cutinites and telalginites, the emphasis being on the results of ^{13}C NMR spectra and Py.-g.c./m.s.

By definition liptinite is recognisable as fossilised tissue. It must therefore consist of chemical structures which have resisted or escaped bacterial and chemical attack and remained, preserving the morphology of the original tissue throughout diagenesis (Ref. [68] and other references therein). The maceral, resinite appears to derive from the fluid (sap) of certain plants. Its structure seems to vary [48], though, by analogy with recent plants, isoprenoids should be prominent [69]. Sporinite, cutinite and alginite, major components of liptinite, all derive from outer cell membranes or walls which, while being permeable to a greater or lesser extent and embracing chloroplasts, have the precise function of protecting the cell contents from attack by chemicals and microorganisms. Unsurprisingly, therefore, not only do these liptinites appear to fluoresce similarly, the chemical structures of sporinite, cutinite and alginite, as revealed by ^{13}C NMR and Py.-g.c./m.s. are similar. Each maceral generates *n*-alkanes and *n*-alk-1-enes on pyrolysis and usually also alkyl benzenes, alkyl phenols and some alkyl naphthalenes. ^{13}C NMR generally reveals aromaticities of 0.2–0.4, though the alkyl aromatics are often the most dominant of the products generated by pyrolysis. Investigation of the alkanes extractable from the liptinite macerals (bitumens) as well as those generated by pyrolysis has distinguished distributions characteristic of marine and terrigeneous (higher plant) vegetation, the latter generally being indicated by the prominence of alkanes longer than C_{23} [46,64]. Recent research has sought the origin of the alkanes and alkenes in aliphatic or lipoidal biopolymers expected to be major constituents of the outer cell membrane [64,67,69]. The source of the alkyl benzenes has tentatively been attributed to carotenes, which are often present in significant concentrations in the cell membranes of microalgae [70] and to the diagenesis of unsaturated fatty acids [71], though toluene, styrene, methyl and ethyl phenols, and indoles might also derive from the aromatic amino acid residues of those proteins which facilitated activated diffusion across the cell membrane as well as those which support the photosytem in the chloroplasts. Although not derived from lignin, the phenols may be

derived from of other biomolecules in terrigeneous [48] and aquatic plants [69]. Contemporary studies emphasise the correlation between recognisable structures of plant (and animal [72]) fragments and chemically inert (non-hydrolysable) material, difficult to extract [72,73].

4.7.2. Sporinites

Sporinites arise from rather impermeable cell wall material, often termed sporopollenin, whose aromatic component may have derived from carotenes and plant phenols (Ref. [74] and references therein). Investigations consistent with this and with the general discussion above nevertheless reveal variations in the observed chemical structure. Davis et al. [49] observed much of Carboniferous sporinites to be unextractable in pyridine, difficult to degrade and to possess an aromaticity of 0.5–0.6. They concluded that the pyridine insoluble material was polymeric with an aliphatic skeleton on which benzene, often phenolic, rings were pendant. Subsequently, biopolymeric material yielding polyphenols on pyrolysis has been found in the outer walls of fossilised seeds from aquatic plants [69]. More recently, Collinson et al. [48] studying sporinites having aromaticities of 0.4, observed that whereas the most prominent peaks generated by Py.-g.c./m.s. were individual aromatic compounds, the most intense *n*-alkanes were usually C_8 and C_9, although significant intensities were observed till about *n*-C_{14}.

4.7.3. Cutinites

One expects plant cuticles to be more permeable than plant spores and seeds. ^{13}C NMR shows fossil cutinite to have aromaticities of only 0–0.2 [48]. Though C_{10}–C_{12} *n*-alkanes and alkenes are generated in the largest quantities by Py.-g.c./m.s., all chain lengths up to and beyond C_{30} have been observed [48,72]. These aliphatics appear to have been generated from a saponifiable biopolymer and lipids have indeed been observed in recent plant cuticles [73]. Accordingly, it has been suggested that the aliphatic material in fossil cutinite, which has resisted attack by chemicals and microorganisms, has been formed by the polymerisation of esterified fatty acids during diagenesis [72]. Despite the low aromaticities of cutinite, alkyl benzenes and phenols have been observed to dominate the results of Py.-g.c./m.s. [48,73].

4.7.4. Alginites

Telaginites, notably Tasmanite and Kukersite, also possess low aromaticities and, whereas the alkanes generated by Py.-g.c./m.s. are most intense at C_9, the intensities decline dramatically at higher carbon numbers [48]. The lamalginite oil shale and the marinite sapropel reported here had aromaticities of about 0.2 (Table 3) and Py.-g.c./m.s. generated *n*-alkanes and *n*-alk-1-enes with maximum intensities around C_{15}. The intensities of alkanes with higher carbon numbers were low.

These results should be interpreted with caution. The aquatic origin of the sapropels and the oil shale, both of them alginites, may partly explain the comparative absence of long chain alkanes characteristic of higher plants generated by Py.-g.c./m.s. but the same explanation cannot be true of the relative absence of higher *n*-alkanes noted in the Py.-g.c./m.s. of sporinite and cutinite [48,72]. The general dominance of C_9–C_{15} alkanes and alkenes in pyrolysates from liptinites might result from cracking of the higher carbon numbers either during Py.-g.c./m.s. or possibly during catagenesis. It will be recalled that, after flash pyrolysis, 50% of the Black Sea sapropel remained as a non-volatile, tarry residue and that flash pyrolysis of *n*-hexadecanoic acid generated several alkanes.

Algae might be expected to possess more porous cell membranes than either spores or cuticles. The lipoidal material in the cell walls is the source of the aliphatics observed by Py.-g.c./m.s. of our lamosites. We have already mentioned the evidence [64,67; Section 4.6.3] that the cell walls of micro algae—but not apparently dinoflagellates or diatoms—are constituted of algaenans, polymerised long chain esters stabilised by ether cross links. Microalgae can contain significant concentrations of carotenes, which may be the source of the alkyl aromatics liberated on pyrolysis [70] (though not of the alkyl phenols). The observed aromaticity of ~0.2 implies the presence of one benzene ring for every twenty four aliphatic carbon atoms. There being very little bitumen in the Black Sea sapropels, the benzene rings are either chemically bound to the algaenans or have become trapped within the polymerised algaenan matrix. This is consistent with the suggestion (Section 4.3) that the benzene rings are able to transfer light energy to the residues of the algal photosystems originally associated with the algaenan.

5. General discussion and conclusions

The observations presented here, placed within the background of previous work, yield a detailed description of the continuing formation of a source rock from phytoplankton deposited on the Black Sea bed that appears in complete conformity with current theories. Deposition of Unit 2 was initiated 7000–7700 years ago by the abrupt pouring of the Mediterranean into the fresh water, lacustrine, Holocene Black Sea [18]. Deposition of sapropels accompanied the development of anoxia [20]. Sapropel formation ceased about 3800 years later when the euphotic zone of the Black Sea became sufficiently saline to permit the growth and subsequent deposition of coccoliths.

The sapropels were deposited as sapropel–varve couples, each couple containing material chemically similar to Type 1 kerogen consisting of an approximately 50 μm thick layer of impure marinite [40], containing small amounts of telalginite and occasional inclusions of sporinite, resinite, cutinite, huminite and inertinite in a ground mass of mineral matter. The sapropels fluoresced (Emission maxima at 500–550, ~600 and ~650 nm with excitation at 365 nm) and the

products of their flash pyrolysis consisted mainly of alkanes (16%), alkenes (28%), alkyl benzenes (35%), alkylated naphthalenes and some phenols. Pyrolysis in the presence of tetramethylammonium hydroxide showed much of the alkanes to derive from aliphatic carboxylic acids typical of those in the lipid membranes of phytoplankton. The aromaticity of the sapropels was ~0.2. It has been suggested that in Type 1-2 kerogens such aromatic material may have been formed from the carotenes and aromatic carotenoids originally present [70]. Carotenes occur in significant concentrations in microalgae and may account for the green (~500–550 nm emission) fluorescence of the sapropels.

Each layer of marinite appears to originate from the annual primary production in the Holocene Black Sea. Most of the particulate organic matter in the Black Sea could be expected to have consisted mainly, as now [75], of carbohydrates, proteins, lipids and carotenes together with small amounts of chlorophyll pigments and nucleic acids. Much of this material experiences oxic and anoxic decay in the water column and only lipids and some protein residues can be observed in present particulate organic matter below the euphotic zone [75]. Rapidly sedimenting organic particulates still containing residues of carbohydrates and proteins will have been deposited on the sea floor—together sometimes with allochthanous material [36], though little was observed in the present sapropels. There is little evidence of carbohydrate or protein residues in the sapropels and these compounds must have been consumed by the abundant bacteria in the surface sediment. The sapropels are derived from the less labile and less reactive lipoidal material in the outer cell wall or membrane of the phytoplankton, a process which has been termed selective preservation [76]. In this way kerogen formed as sapropels a few thousand years old is already very similar chemically to that constituting a Type 1 kerogen oil shale a few million years old.

The sapropels contain up to 2 wt% of sulphur and the dominant organic sulphur forms are mono-sulphides that probably have arisen from the combination of sulphur nucleophiles with unsaturated lipids and carotenes [48,55,58]. The low C–S bond energy would facilitate the formation of crude-oil and, in particular, alkyl aromatics during subsequent catagenesis [52,77]. In conformity with increase of maturity on a van Krevelen diagram, catagenesis will decarboxylate the existing fatty acids to yield alkanes, will increase the aromatisation of carotenes [70], and will dry the organic-rich mud to yield an oil shale.

Rapid pyrolysis of the sapropels gave a tarry residue amounting to about half of the original organic material The yields and composition of the pyrolysis products were little affected by pre-extraction of the sapropel. The species identified are predominately covalently bound to the kerogen matrix. Alginites, cutinites and sporinites all generated varying proportions of the same classes of compound on Py.-g.c./m.s. These liptinites behave similarly on pyrolysis and they yield similar ^{13}C NMR spectra but they differ in the structures of their polymeric matrix which, in each liptinite, has derived from the outer cell membrane of the corresponding (usually) plant tissue.

Acknowledgements

This work has been supported generously by the Science Research Councils of both Turkey (TUBITAK) and Italy (CNR). The gravity cores were a gift from the Turkish Petroleum Corporation (TPAO). We are grateful to Professor Ilkay Salihoglu (METU) and to Karl Ottenjahn (Geologisches Landesamt, Nordrhein-Westfallen, Krefeld, Germany) for their encouragement. The investigation formed a small part of NATO's Science for Stability Program.

References

[1] Bertrand, Renault, 1892, Renault, 1899, Potonie, 1910, cited by Hendricks TA. In: Lowry HH, editor, The chemistry of coal utilisation. New York: Wiley, vol. 1, 1945. p. 1.
[2] Bodoev NV, Guet J-M, Gruber R, Dolgopolov NI, Wilhelm J-C, Bazarova O. Fuel 1996;75:839.
[3] Boudreau BP, Canfield DE, Mucci A. Limnol Oceanogr 1992;37:1738.
[4] Luettig G. Telma 1996;26:27.
[5] Pruysers PA, de Lange GJ, Middleburg JJ. Mar Geol 1991;100:137.
[6] Orlov DS, Rudakova IP, Ammosovia YaM. Geokhimya 1996;2:160.
[7] Kidd RB, Cita MB, Ryan WBF. In: Hsu KJ, Montadert L, editors. Deep sea drilling project, vol. 42A. Washington, DC: US Govt. Printing Office, 1978. p. 421.
[8] Ross DA, Neprochnov YP, et al. Deep sea drilling project, vol. 42B. Washington, DC: US Govt. Printing Office, 1978.
[9] Piskaln CH. In: Murray JW, Izdar E, editors. Black sea oceanography, Dordrecht: Kluwer Scientific, 1991. p. 293.
[10] Simoneit BRT. In: Degens ET, Ross DA, editors. The black sea—geology, chemistry and biology. Am Assoc Petrol Geol, Memoir, Tulsa, OK, vol. 20, 1974. p. 477.
[11] Simoneit BRT. In: Ross DA, Neprochnov YP, editors. Deep Sea Drilling Project, vol. 42B. Washington, DC: US Govt. Printing Office, 1978. p. 749.
[12] Wakeham SF, Beier JA, Clifford CH. In: Murray JW, Izdaar E, editors. Black sea oceanography, NATO ASI Dordrecht: Kluwer Academic, 1991. p. 319.
[13] Wakeham SF, Beier JA. Deep-Sea Res 1992;38 (suppl. 2):S943.
[14] Huc AY, Durand B, Monin JG. In: Ross DA, Neprochnov YP, editors. Deep sea drilling project, vol. 42B. Washington, DC: US Govt. Printing Office, 1978. p. 421.
[15] Didyk BM, Simoneit BRT, Braswell SC, Eglinton G. Nature 1978;272:216.
[16] van de Meent D, Brown SC, Philp RP, Simoneit BRT. Geochim Cosmochim Acta 1980;44:999.
[17] Putun E, Akar A, Ekinci E, Frere B, Bartle KD, Snape CE, Citiroglu M. J Petrol Geol 1991;14:459.
[18] Ryan WBF, Piman III WC, Major CO, Shikmus K, Moskalenko V, Jones GA, Dimitrov P, Gorur N, Yuce H. Mar Geol 1997;138:119.
[19] Atalay I. The paleogeography of the near east. Bornova, Izmir, Turkey: Ege University Press, 1992.
[20] Wilkin RT, Arthur MA, Dean WE. Earth Planet Geol Lett 1997;148:517.

[21] Calvert SE, Karlin RE, Toolin LJ, Donahue DJ, Southon JR, Vogel JS. Nature 1991;350:692.
[22] Sun M-Y, Wakeham SF. Geochim Cosmochim Acta 1994;58:3395.
[23] Arthur MA, Dean WE, Neff ED, Hay BJ, King J, Jones G. Biogeochem Cycles 1994;8(2):195.
[24] Jones GA, Gagnon AR. Deep-Sea Res 1994;41:325.
[25] Bukry D. In: The black sea—geology, chemistry and biology. Degens E, Ross D, editors. Am. Assoc. Petrol. Geol., Memoir 20, Tulsa, OK, 1974. p. 253.
[26] Hay BJ, Arthur MA, Dean WE, Neff ED, Honjo S. Deep-Sea Res 1991;38:S1211.
[27] Kubilay N, Saydam AC. Personal Communication, 1995.
[28] Muller P. Methods in sedimentary petrology. Germany: Hafner, 1967. p. 216.
[29] Ottenjahn K, Teichmuller M, Wolf M. In: Alpern B, editor. Petrographie de la matiere organique des sediments, relation avec la Paleotemperature et le potential petrolier, 1975. p. 67.
[30] Teichmuller M, Ottenjahn K. Erdol und Kohle 1977;30:387.
[31] Teichmuller M, Wolf M. J Microsc 1977;109:49.
[32] Robert P, Int J. Coal Geol 1981;1:101.
[33] Crelling JC. J Microsc 1983;132:132.
[34] Teerman SC, Crelling JC, Glass GB, Int J. Coal Geol 1987;7:315.
[35] Hittachi, Instrumentation Manual Model, F3000, 1992.
[36] Ergin M, Gaines A, Galletti GC, Chiavari G, Fabbri D, Yucesoy-Eryilmaz F. Appl Geochem 1996;11:711.
[37] Fabbri D, Chiavari G, Galletti GC. J Anal Appl Pyr 1996;37:161.
[38] Acholla FV, Orr WL. Energy and Fuels 1993;7:406.
[39] Mitchell SC, Snape CE, Garcia R, Ismail K, Bartle KD. Fuel 1994;73:1159.
[40] Schrader H-J, Jouse AP, Mukhina VV, Koreneva EV, Kartashova GG, et al. Deep sea drilling project, vol. 42B. Washington, DC: US Govt. Printing Office, 1978. p. 789, 903, 951.
[41] Stoffers P, Muller G. Deep sea drilling project, vol. 42B. Washington, DC: US Govt. Printing Office, 1978. p. 373.
[42] Hutton AC. In: Snape CE, editor. Composition, geochemistry, and conversion of oil shales, Dordrecht: Kluwer Academic, 1995. p. 17.
[43] Karayigit AI, Whately MKG, Int J. Coal Geol 1997;34:131.
[44] Van Bergen PF, Janssen NMM, Alferink M, Kerp JHF. Meded Rijks Geol Dienst 1990;45:9.
[45] Mopper K, Kieber DJ. Deep-Sea Res 1991;38:S1021.
[46] Blumer M, Guillard RRL, Chase T. Marine Biol 1971;8:183.
[47] Sinninghe Damste JS, Wakeham SG, Kohnen MEL, Hayes JM, de Leeuw JW. Nature 1993;362:827.
[48] Collinson ME, van Bergen PF, Scott AC, de Leeuw JW. In: Scott AC, Fleet AJ, editors. Coal and Coal bearing strata as oil-prone source rocks, Geological Society Special Publication, vol. 77. 1994. p. 31.
[49] Davis MR, Abbott JM, Cudby M, Gaines AF. Fuel 1988;67:960.
[50] Hemsley AR, Chaloner WG, Scott AC, Groombridge CJ. Ann Botany 1992;69:545.
[51] Snape CE, Ladner WR, Bartle KD. Anal Chem 1979;51:2189.
[52] Maroto-Valer MM, Love GD, Snape CE. Energy and Fuels 1997;11:539.
[53] Sinninghe Damste JS, Eglinton TI, de Leeuw JW, Schenck PA. Geochim Cosmochim Acta 1989;53:873.
[54] Sinninghe Damste JS, Eglinton TI, Rijpstra WIC, de Leeuw JW. In: Orr WL, White CM, editors. Geochemistry of sulphur in fossil fuels, ACS Symposium Series 429 Washington, DC: ACS, 1990. p. 486.
[55] Valisolalo J, Perkins N, Chappe B, Albrecht P. Tetrahedron Lett 1984;25:1183.
[56] Gelin F, Kok MD, de Leeuw JW, Sinninghe Damste JS. Org Geochem 1998;29:1837.
[57] Sinninghe Damste JS, de Leeuw JW. Org Geochem 1990;16:1077.
[58] Davidson RM. Fuel 1994;73:988.
[59] Brown SD, Sirkecioglu O, Snape CE, Eglinton TI. Energy and Fuels 1997;11:532.
[60] Eglinton TI, Irvine JE, Vairavamurthy A, Zhou W, Manowitz B. Org Geochem 1993;22(3–5):781.
[61] Gonenc ZS, Gibbins JR, Kathaklakis IE, Kandiyoti R. Fuel 1990;69:383.
[62] Carmo AM, Stankiewicz BA, Mastalerz M, Pratt LM. Org Geochem 1997;26:587.
[63] Love GD, Snape CE, Fallick AE. Org Geochem 1998;28:797.
[64] Gelpi E, Schneider H, Mann J, Oro T. Phytochemistry 1970;9:603.
[65] Youngblood WH, Blumer M. Mar Biol 1973;8:190.
[66] Volkman JK, Barrett SM, Blackburn SI, Mansour MP, Sikes EL, Gelin F. Org Geochem 1998;29:1163.
[67] Blokker P, Schouten S, van den Ende H, de Leeuw JW, Hatcher PG, Sinninghe Damste JS. Org Geochem 1998;29:1543.
[68] Stasiuk LP. Org Geochem 1999;30:1021.
[69] De Leeuw JW, van Bergen PF, van Aarssen BGR, Gatellier J-PLA, Sinninghe Damste JS, Collinson ME. Phil Trans R Soc London 1991;B333:329.
[70] Hartgers WA, Sinninghe Damste JS, de Leeuw JW. Geochim Cosmochim Acta 1994;58:1759.
[71] Ellis L, Fisher SJ, Singh RK, Alexander R, Kagi RI. Org Geochem 1999;30:651.
[72] Stankiewicz BA, Scott AC, Collinson ME, Finch P, Mosle B, Briggs DEG, Evershed RP. J Geol Soc 1998;155:453.
[73] Mosle B, Finch P, Collinson ME, Scott AC. J Anal Appl Pyr 1997;40/41:585.
[74] Hemsley AR, Chaloner WG, Scott AC, Groombridge CJ. Ann Botany 1992;69:545.
[75] Chiavari G, Coban Y, Fabbri, D, Galletti G, Tugrul S. Org Geochem 2000 (in press).
[76] Tegelaar EW, de Leeuw JW, Derenne S, Largeau C. Geochim Cosmochim Acta 1989;53:3103.
[77] Hunt JM, Lewan MK, Hennet R. Bull Am Assoc Petrol Geol 1991;75:795.